Int. J. Morphol.,
42(6):1464-1473, 2024.

Human Adipose-Derived Stem Cells Promote Axonal Growth and Survival of Rat Retinal Ganglionic Cells Through Anti-Inflammatory, Anti-Oxidant, Anti-Apoptotic, and Paracrine Stimulation via the PI3K/Akt Pathway

Las Células Madre Derivadas de Tejido Adiposo Humano Promueven el Crecimiento Axonal y la Supervivencia de las Células Ganglionares de la Retina de Rata Mediante Estimulación Antiinflamatoria, Antioxidante, Antiapoptótica y Paracrina a Través de la vía PI3K/Akt

Guiyan Mi[1]; Bingqing Li[2,3]; Xuewu Gong[4]; Jing Wu[4]; Yu Zhang[4]; Li Ma[4] & Lijie Sheng[4]

MI, G.; LI, B.; GONG, X.; WU, J.; ZHANG, Y.; MA, L. & SHENG, L. Human adipose-derived stem cells promote axonal growth and survival of rat retinal ganglionic cells through anti-inflammatory, anti-oxidant, anti-apoptotic, and paracrine stimulation via the PI3K/Akt pathway. *Int. J. Morphol., 42(6)*:1464-1473, 2024.

SUMMARY: The present study aimed to investigate the in vitro effect of human adipose derived stem cells (hADSCs) and their secretions on viability of retinal cells and the axonal growth. After isolation, the rat retina was kept in containers covered with poly-D-lysine/laminin, after preparing the supernatant of hADSCs, the retina along with cells and hADSCs conditioned medium (CM) were co-cultured. The viability was assessed by 3-[4,5-dimethylthiazol-2-yl]-2,5 diphenyl tetrazolium bromide (MTT) assay at days 1, 7 and 14, and axonal growth of retinal cells was analyzed by Image J software using Neurite J plug-in. The expression of PI3K/Akt pathway genes and its proteins were evaluated through real-time polymerase chain reaction (PCR) and western blot, respectively. Anti-oxidant effects of hADSCs and their CM were measured by measuring the retina cells level of thiobarbituric acid reactive substance (TBARS), ferric reducing ability of plasma (FRAP) and glutathione (GSH). Brain-derived neurotrophic factor (BDNF), neurotrophin-3 (NT-3) and NT-4 in the CM were measured by enzyme-linked immunosorbent assay (ELISA). The CM contained high levels of BDNF, NT-3 and NT-4 compared to the control group. The expression of genes and proteins of the PI3K/Akt pathway along with levels of TBARS, FRAP and GSH was also increased in the group of hADSCs and their CM compared to the control group. The results of this study showed that hADSCs can increase the axonal growth and survival of rat retinal cells through anti-inflammatory, anti-apoptotic, and paracrine stimulation, as well as through the PI3K/Akt pathway.

KEY WORDS: Adipose-Derived Stem Cells; Retina; Anti-oxidant; PI3K/Akt pathway; Co-culture.

INTRODUCTION

Axonal regeneration of retinal neural cells faces various challenges, such as inhibition of myelinating cells (oligodendrocytes and Schwann cells), the formation of glial scars, and the presence of macromolecules like extracellular proteins (Aladdad & Kador, 2019; Eastlake *et al*., 2020). Various strategies, such as gene therapy, laser therapy, and the utilization of stem cells, have been explored for retinal regeneration (Curcio & Bradke, 2018). Among these strategies, stem cells have gained significant attention in recent years. Stem cells possess the remarkable ability to proliferate, regenerate, and differentiate into diverse cell types. They are categorized based on various parameters, including their origin and potential for differentiation, into embryonic stem cells (ESCs), adult stem cells (ASCs), and induced pluripotent stem cells (Achberger *et al*., 2019; Han *et al*., 2020). The ESCs, derived from the embryonic inner cell mass, exhibit pluripotency and high proliferation capacity but are limited in their usage due to ethical considerations (Zakrzewski *et al*., 2019).

[1] Department of Ophthalmology, Chifeng Ningcheng County Central Hospital, Chifeng Inner Mongolia, 024200, China.
[2] Beijing Tongren Eye Center, Beijing Tongren Hospital, Capital Medical University Beijing Institute of Ophthalmology, Beijing Key Laboratory of Ophthalmology and Visual Sciences, China.
[3] Zhang Jiakou Aier Eye Hospital, Zhang Jiakou Hebei, 075000, China.
[4] Department of Ophthalmology,The Second Affiliated Hospital of Qiqihar Medical University,Qiqihar Heilongjiang,161006, China.
Guiyan Mi and Bingqing Li are co-first authors, they contributed equally to this work.
FUNDING: [1]Science and technology plan of Heilongjiang Provincial Health Commission (20230707020510). [2] 2024 Qiqihar City Science and Technology plan joint guidance project (LSFGG-2024046).

Received: 2024-06-28 Accepted: 2024-07-17

The ASCs belong to a category of stem cells that can be derived from various sources, including bone marrow, adipose tissue, and neural tissue. Among these sources, adipose-derived stem cells (ADSCs) are particularly favored due to their accessibility and abundance in adipose tissue, making them suitable for patient use (Ye *et al*., 2018; Karagiannis *et al*., 2019). The primary role of ADSCs is to sustain the viability of living organisms and promote tissue regeneration. These cells exhibit extensive self-renewal capabilities. The ASCs can be isolated from different tissues, such as bone marrow, adipose tissue, umbilical cord, and dermis (George *et al*., 2020). Notably, ADSCs possess a significant characteristic of secreting various growth factors, including neurotrophic factors (NTFs) or factors that enhance neuronal viability. These growth factors play a critical role in facilitating axonal regeneration and preventing neuronal apoptosis (Ong, Chakraborty & Sugii, 2021).

The NTFs exert their influence on both neuronal and non-neuronal cells. Notable examples of these factors include neurotrophins like ciliary neurotrophic factor (CNTF) and fibroblast growth factor (FGF), which regulate neuronal cell differentiation and viability and play a pivotal role in synaptic formation within the central nervous system. Furthermore, a variety of neurotrophins, such as brain-derived neurotrophic factor (BDNF), glial-derived neurotrophic factor (GDNF), NTF-3, NTF-4, NTF-5, and nerve growth factor, are classified based on their receptor tyrosine kinase (TrkB, C) (Skaper, 2018; Jiang *et al*., 2019; Hunsberger *et al*., 2022). The conditioned medium (CM) derived from ADSCs contains neurotrophic and neuroprotective factors, which can promote axonal growth and enhance the viability of ganglion cells (Metcalfe, 2019). Hence, this study aimed to investigate the co-culture effect of human ADSCs (hADSCs) and their ASCs CM on the rat retina and analyze the axonal growth rate and viability of retinal cells through anti-inflammatory, anti-apoptotic, and paracrine stimulation, as well as through the PI3K/Akt pathway.

MATERIAL AND METHOD

Isolation of hADSCs. In this study, subcutaneous adipose tissue was obtained from 27 years old -young patient who provided consent for the surgery. The tissue collection process adhered to sterile conditions, and it was subsequently transferred to the laboratory. To prepare the tissue, it was washed with phosphate-buffered saline (PBS), and any cell debris and blood cells were isolated by mechanically chopping the tissue with a sterile scalpel. Subsequently, a concentration of 0.075 % collagenase I enzyme (Gibco BRL, Rockville, MD) was added for a 30-min incubation period. After this, fetal bovine serum (FBS) 10 % + Dulbecco's modified Eagle's medium (DMEM) (Gibco BRL, Rockville, MD) was added. The conditioned medium was then collected after centrifugation, while the cell sediment was cultured in T25 flasks with culture medium at 37 °C and 5 % CO_2. The culture medium was changed after 48 h, and passage was performed once the culture dish reached approximately 80 % cell confluence. Passage 3-4 cells were utilized for co-culture in this study (Fuoco *et al*., 2020).

Preparation of ASCs CM. To prepare the CM, hADSCs from passages 3 and 4 were cultured at a density of 10^5 cells/ml for 72 h. The hADSCs CM was isolated by centrifugation at 10000 *g* for 10 min and then passed through a filter (Amicon Ultra-15, MERK, Germany). The resulting solution was then centrifuged at 12000 *g* for 12 min, and the hADSCs CM was concentrated 30 times and stored at -70 °C until use (Fig. 1) (Packer *et al*., 2018).

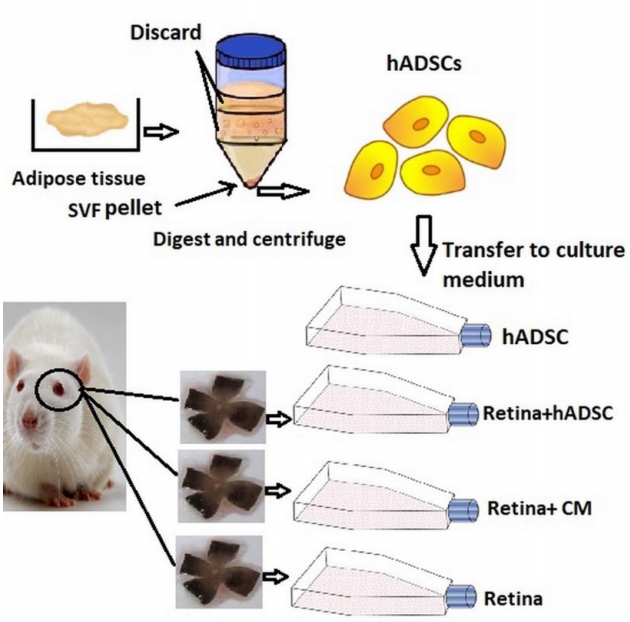

Fig. 1. Study design and grouping.

Preparation of rat retina. To isolate the rat retina, two-month-old Wistar rats (eighteen in three groups/n=8 per group) were utilized. The rats were anesthetized [using xylazine 2 % (Sigma, St. Louis, MO, USA) at a dose of 80 mg/kg] followed by anesthesia [utilizing ketamine 10 % (Sigma, St. Louis, MO, USA) at a dose of 40 mg/kg], and their eyeballs were dissected. Subsequently, the eyes were rinsed with PBS, and upon removing the anterior segment of the eye and isolating the vitreous body, the posterior segment was positioned on the floor of a container with the retinal ganglion cell (RGC) facing upwards. Four longitudinal sections were then prepared (Fig. 2a). Following this, the retina (with the ganglion layer facing upwards) was isolated using a brush under a stereomicroscope (Olympus SZX12, Shinjuku, Tokyo, Japan). The isolated retina was

placed in a 24-well culture dish coated with 400 µl of poly-D-lysine/laminin (PDLL; Sigma, St. Louis, MO). Additionally, 200 µl of retinal culture medium (L-glutamine, Penicillin/streptomycin, non-essential amino acids, N2, DMEM/F12, and B27) was added to the culture dish (Koh *et al*., 2019). The ethics committee of the second affiliated hospital of Qiqihar Medical University, Qiqihar Heilongjiang, China supervised the maintenance, behavior and sacrifice under national and international standards protocols according to NIH Publication, 1996 and European Communities Council Directive of November 24, 1986 (approval number: 2022- kj0076578).

Case groups

The study comprised three experimental groups as described below:

1. Rat retinal cells control group: This group entailed the culture of retinal cells without hADSCs (Fig. 2b-A).

2. Rat retinal and hADSCs direct co-culture group: This group involved the culture of retinal cells and hADSCs (retina/ADSCs) (Fig. 2b-B).

3. Rat retinal and hADSCs indirect co-culture (CM co-culture) group: This group involved the co-culture of retinal cells and hADSCs CM (retina/CM) (Fig. 2b-C) (Pereiro *et al*., 2018; Dezfuly *et al*., 2022).

Direct co-culture. Equal segments of retinal tissue were cultured in 24-well culture dishes that were coated with PDLL (400 µl) for 24 h. Following this, a cell suspension containing 1000 cells/µl of ADSCs was transferred to the RGCs, with a volume of 2 µl (Pereiro *et al*., 2018; Dezfuly *et al*., 2022).

Indirect co-culture. Equal segments of retina were cultured in 24-well culture dishes that were coated with PDLL (400 µl) for 24 h. Subsequently, a 10 % concentrated hADSCs CM was added to the retina. The cell viability rate in both direct and indirect co-cultures was evaluated at days 1, 7, and 14 using the [4,5-dimethylthiazol-2-yl]-2,5 diphenyl tetrazolium bromide (MTT) assay, while axonal growth was assessed at day 14 using the immunohistochemistry (IHC) assay (Pereiro *et al*., 2018; Dezfuly *et al*., 2022).

Analysis of cell viability. The MTT assay was utilized to determine cell viability. For this purpose, 400 µl of DMEM and 40 µl of MTT were added to the cultured cells in the 24-well plates after removing the hADSCs CM. The cells were then incubated for 4 h. followed by the removal of the MTT solution and the addition of 400 µl of dimethyl sulfoxide (DMSO). The absorption rate at a wavelength of 540 nm was subsequently measured after 20 min (Ibán-Arias *et al*., 2019).

Axonal growth analysis. Axonal growth was measured using the immunofluorescence technique with the b-tubIII

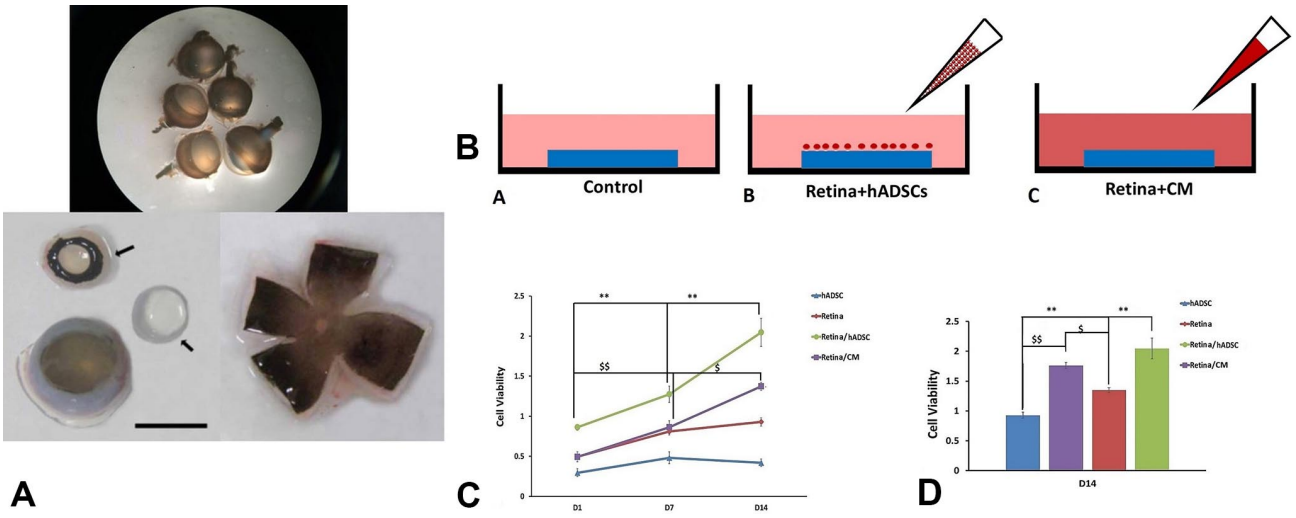

Fig. 2. (a) Four longitudinal sections were prepared from the posterior segment and retina was isolated as ganglion layer was upward. (b) Schematic of case groups. Indirect co-culture (Retina+CM), direct co-culture (Retina+hADSCs) and control (Retina) groups. Cell viability analysis in hADSCs, indirect co-culture (Retina+CM), direct co culture (Retina+hADSCs), and control (Retina) groups. (c) Comparison of MTT results at days 1, 7 and 14 in different study groups. ** ($p<0.01$): Comparison of Retina/hADSC in day 14 with 1 and 7 days. $ ($p<0.05$) and $$ ($p<0.01$): Comparison of Retina/CM in day 14 with 1 and 7 days. (d) Comparison of MTT results at day 14 between studies groups (B). ** ($p<0.01$): Comparison of Retina/hADSC with control (Retina) and hADSCs groups. $ ($p<0.05$) and $$ ($p<0.05$): Comparison of Retina/CM with hADSC and Retina.

antibody. The number of process intersections was determined by measuring lines using the Neurite J plug-in in the Image J software. For the immunohistochemical analysis, the primary antibody utilized was the human monoclonal antibody β-tubIII (Mab3402 Chemicon, Nippon Chemi-Con, Japan) at a concentration of 1/200, while the secondary antibody employed was the goat polyclonal antibody fluorescein isothiocyanate (FITC) anti-mouse IgG (ab97022, abcam, US) at a concentration of 1/200. In the immunohistochemical analysis, the cells were cultured on cover glass. The culture medium was removed, and the cells were washed with PBS without calcium and magnesium. They were then fixed at room temperature with 4 % paraformaldehyde for 30 min. Subsequently, the cells were washed twice with PBS every five min and incubated in 0.2 % Triton 100X at 37 °C for one hour. Following this, the cells were incubated overnight in darkness with the primary antibodies [diluted in PBS and bovine serum albumin (BSA) 10 mg/ml]. After the incubation with the primary antibody (b-tubIII), the cells were incubated with the diluted secondary antibody (FITC anti-mouse IgG) (diluted in PBS and BSA 5 mg/ml). 4',6-diamidino-2-phenylindole (DAPI) (3 ng/ml) was added, and the cells were incubated at room temperature for 3 min before being washed with PBS. The cover glass was then removed, and the slides were mounted with enthlan medium and analyzed using a fluorescent microscope (Ahmed *et al*., 2019).

Conditioned medium levels of GDNF, BDNF, neurotrophin-3 (NT-3) and NT-4. To measure the level of BDNF (catalog number: ab213899), GDNF (catalog number: ab171178), NT-3 (catalog number: ab213905), and NT-4 (catalog number: ab150437) in the culture media, Abcam colorimetric sandwich-based enzyme-linked immunosorbent assay (ELISA) kits were used according to standard protocols (Abcam, United States) (Zhao *et al*., 2021).

Antioxidant parameters

Total antioxidant capacity (TAC). The total antioxidant capacity assay was performed using the colorimetric BT-laboratory kit (catalog number: SH0242; BT Laboratory, China) based on the ferric reducing antioxidant power (FRAP) method, following the recommendations and guidance of the manufacturer. The assay involved the conversion of Fe^{3+}- tripyridyltriazine (TPTZ) to Fe^{2+}-TPTZ, and the absorbance was read at 593 nm using a JASCO BIO spectrophotometer (model number: V-630 Bio; JASCO, US) (Verma *et al*., 2019).

Lipid peroxidation level. The level of lipid peroxidation in the cells was assessed using thiobarbituric acid reactive substances (TBARS). The cell contents were centrifuged at 10,000 *g* for 10 min at 4 °C, and 100 µl of lysis buffer was added to 10^6 cells. The mixture was then subjected to another centrifugation at 10,000 *g* for 10 min at 4 °C, and the resulting supernatant was transferred to a tube containing TBARS solution (100 µl). After incubation at 37 °C for 30 min, the mixture underwent centrifugation once again at 10,000 *g* for 10 min at 4 °C. The absorbance was measured at a wavelength of 593 nm using an ultraviolet (UV)-visible spectrophotometer (model number: V-630 Bio; JASCO, US) (Verma *et al*., 2019).

Glutathione (GSH) level. The Cell Signal Cellular Glutathione Detection Assay Kit (catalog number: 13859; Cell Signal, United States) was used to measure the cellular reduced glutathione (GSH) level. First, the culture medium was aspirated, and 100 µl of lysis buffer was added to each cell dish, followed by incubation at 4 °C for 10 min. The mixture was then centrifuged at 10,000 *g* for 5 min at 4 °C, and the resulting supernatant was immediately transferred to a 96-well plate. Then, 50 µl of the kit's working solution and 50 µl of the kit's assay buffer were added to each well. After incubation at 37 °C for 10 min and centrifugation at 10,000 *g* for 10 min at 37 °C, the absorbance was measured at 460 nm using a UV-visible spectrophotometer (model number: V-630 Bio; JASCO, US) (Verma *et al*., 2019).

Real-time polymerase chain reaction (PCR) assay

Total RNA extraction. To extract RNA, the culture medium was aspirated, and 10^6 cells were washed with ice-cold PBS (1 ml). Next, 1 ml of TRIzol was added to the cells, and the mixture was incubated at 25 °C for 2 min. The TRIzol/cell lysate was then transferred to a 2 ml tube, and 250 µl of chloroform was added. After incubating for 2 min at 25 °C, the mixture was centrifuged at 10,000 *g* for 5 min. The top layer was aspirated and transferred to a new 2 ml tube, and 550 µl of isopropanol was added to it. After incubation for 2 min at 25 °C, the mixture was centrifuged at 12,000 *g* for 20 min. The top layer containing isopropanol was removed, and 1 ml of 75 % ethanol was added to the resulting pellet. After incubating for 1 min at 25 °C, the mixture was centrifuged at 10,000 *g* for 5 min. Finally, the ethanol was extracted, and 10 µl of deionized water was added to the resulting pellet, which was then stored at -20°C (Prendergast *et al*., 2018).

cDNA synthesis and quantitative real-time PCR (qPCR) for expression of GLUT-4, AKT, PI3K and PTEN. The Biotechrabbit™ cDNA Synthesis Kit (catalog number: BR0400404; Berlin, Germany) was used for cDNA synthesis of total RNA according to the manufacturer's protocol (22). In the cDNA synthesis reaction, 2 µl of dNTP Mix (10 mM), 0.5 µl of RNase inhibitor (40 U/µl), 0.5 µl of Oligo/Hexamer primers, 4 µl of 5x cDNA synthesis buffer, and 1 µg of total

RNA were transferred to an RNase-free reaction tube. The cDNA synthesis temperature protocol includes 10 min at 30 °C, 20 min at 55 °C (for Hexamer primer), 20 min at 55 °C, 20 min (for Oligo primer), 99 °C for 5 min (to inactivate the enzyme), and finally, -70 °C until the time of cDNA replication (Bakiu *et al*., 2022).

The primer sequences for PTEN, AKT, PI3K, and GLUT-4 genes were designed using the Primer-3 software (*http://primer3.wi.mit.edu*). The β-actin gene was chosen as the internal reference, and the primer sequences are as follows: β-actin (forward: CCAGCCTTCCTTCTTGGGTA, reverse: CAATGCCTGGGTACATGGTG), GLUT-4 (forward: CTTCCTTCTATTTGCCGTCCTCC, reverse: CATTTTGCCCCTCAGTCATTCTC), PTEN (forward: AGCGTGCGGATAATGACAAG, reverse: GGATTTGATGGCTCCTCTACTG), AKT (forward: TAGGCATCCCTTCCTTACAG, reverse: GCCCGAAGTCCGTTATCT), and PI3K (forward: ACTGAGATGGAGACACGGAAC, reverse: GCATCCAAGGGTCCAGTTAGTG). All primer sequences were blasted using the National Center for Biotechnology Information (NCBI) database (*https://www.ncbi.nlm.nih.gov/tools/primer-blast/index.cgi*).

The gene sequences were amplified using 42 temperature cycles with the help of an Applied Biosystems thermocycler (Applied Biosystems, Quantstudio 1, United States) under the following conditions: 5 min at 50 °C, 15 sec at 95 °C, 1 min at 60 °C, and finally 5 min at 70 °C. After recording the threshold cycle (CT) of genes, the fold change ($2^{-\Delta\Delta CT}$) formula was used to evaluate the relative expression of genes.

Fold change of genes=$2^{-\Delta\Delta CT}$ and $\Delta\Delta C_T = [(C_{T\ Sample} - CT_{\beta\text{-}actin}) - (C_{T\ Sample} - C_{T\ Control})]$ (Huang *et al*., 2019).

Western blotting assay. To evaluate the expression of PI3K/Akt pathway proteins, 20 µl of cell lysates at $1x10^7$ cells per mL were prepared and washed with 200 µl of PBS. Radio-immunoprecipitation assay buffer (200 µl) containing 5 µl of nonyl phenoxypolyethoxylethanol (NP)-40 buffer (0.1 %), 50 µl of Tris-HCl (50 mmol/l), and 50 µl of NaCl (150 mmol/l) was added. After centrifugation (12,000 *g* at 4 °C for 10 min), 50 µg of the mixture was taken and mixed with 5 µl of glycerol (10 %), 5 µl of Tris-HCl (62.5 mmol/l), 5 µl of sodium deoxycholate (0.5 %), and 1 µl of β-mercaptoethanol. The mixture was then incubated for 10 min at 4 °C and loaded onto a sodium dodecyl sulfate (SDS) polyacrylamide gel (10 %) and polyvinylidene fluoride membrane. The membrane was then labeled with anti-GLUT-4 (catalog number: GTX60674; 1:200), anti-PI3K (catalog number: GTX100462; 1:100), anti-PTEN (catalog number: GTX101025; 1:1000), and anti-AKT (catalog number: GTX121937; 1:500) antibodies (GeneTex Bio., US) and incubated for 2 h at 4 °C. Finally, HRP-conjugated secondary antibody was added, and after incubation for 1 h at 37 °C, antibodies were detected using Tween-20 (0.1 %), NaCl (0.15 M), and Tris-buffered saline (25 mM) with the help of Bio-Rad software. Protein signals were detected using enhanced chemiluminescence reagent (e-BLOT company, China) and a charge-coupled device (CCD) camera (LAS-3000, Fuji), and analyzed with Image J software (Zuo *et al*., 2020).

Data analysis. All graphs were created using GraphPad Prism software (version 9; GraphPad Inc, US). Statistical analysis was performed using SPSS software (version 16; SPSS, Chicago, US). One-way analysis of variance (ANOVA) test followed by Tukey's post hoc test was used to compare the results between groups, and $p < 0.05$ was considered statistically significant. Data normality was tested using the Kolmogorov-Smirnov test, and $p > 0.05$ was considered as normal and homogeneous data. All data were repeated three times and expressed as means ± standard deviation.

RESULTS

Cell viability rate. The viability of retinal cells exhibited a significant difference in the direct co-culture group (Retina+hADSC) at day 14 compared to days 1 and 7 ($p<0.01$). Similarly, in the indirect co-culture group (Retina+CM), there was a significant difference in the viability of retinal cells at day 14 compared to day 1 ($p<0.01$) and day 7 ($p<0.05$). However, no significant difference ($p>0.05$) was observed in the viability of retinal cells in the groups utilizing hADSC and retinal cells alone (Fig. 2c).

The viability of retinal cells in all experimental groups exhibited a higher value compared to the control group. The results obtained from the MTT assay at day 14 indicated a significant increase in the viability of retinal cells in the indirect co-culture (Retina + CM) group compared to the control (Retina; $p<0.05$) and hADSC ($p<0.01$) groups. Moreover, the viability of retinal cells in the direct co-culture (Retina + hADSCs) group was significantly higher than the control (Retina; $p<0.01$) and hADSC ($p<0.01$) groups (Fig. 2d).

Axonal growth rate. The stained images obtained after b-Tub III staining were analyzed using the Image J software. The results of this analysis are presented in Figure 2a. Comparative evaluation of the phase-contrast

fluorescent staining (Fig. 3a-A)., β-Tub III staining (Fig. 3a-B), and automatic analysis (Fig. 3a-C, 3a-D) images allowed for the comparison of axonal process growth among all groups. Notably, the growth of axonal processes was observed to be increased in both the indirect co-culture (Retina + CM) and direct co-culture (Retina + hADSCs) groups in comparison to the control group.

The automatic analysis of the number of intersections representing axonal processes and the distance covered by axonal processes allowed for a comparison among the control group (Retina), direct co-culture group (Retina + hADSC), and indirect co-culture group (Retina + CM). The results indicated a significant increase in the number of intersections in both the direct and indirect co-culture groups compared to the control group ($p<0.01$). Furthermore, the number of intersections was found to be significantly higher in the indirect co-culture (Retina + CM) group compared to the direct co-culture (Retina + hADSC) group ($p<0.05$) (Fig. 3b).

Furthermore, the direct co-culture (Retina + hADSCs) and indirect co-culture (Retina + CM) groups exhibited a significant increase in the maximum number (Nmax), distance (RC - maximum distance of neuronal processes), and length (Dmax - longitudinal growth) of processes compared to the control (Retina) group ($p<0.05$ for direct co-culture and $p<0.01$ for indirect co-culture). Moreover, the indirect co-culture (Retina + CM) group demonstrated a significant increase in the Nmax, RC and Dmax of processes compared to the direct co-culture (Retina + hADSCs) group ($p<0.05$) (Fig. 3c).

Secretion medium levels of GDNF, BDNF, NT-3 and NT-4 levels. The assessment of neurotrophic factor levels in the culture media revealed a significant increase in all four factors (GDNF, BDNF, NT-3 and NT-4) in the direct co-culture group (Retina + hADSCs) compared to the control group (Retina; $p<0.01$). Similarly, in the indirect co-culture group (Retina + CM), there was also a significant elevation in the levels of these factors ($p<0.05$) compared to the control group (Retina) (Fig. 4a).

Cells FRAP, TBARS and GSH levels. The evaluation of cellular oxidative stress changes showed that the levels of all three antioxidant parameters (FRAP, TBARS, and GSH) in the direct co-culture group (Retina + hADSCs) significantly increased compared to the control group (Retina; $p<0.01$). Similarly, in the indirect co-culture group (Retina + CM), the levels of all three antioxidant parameters were significantly increased ($p<0.05$) compared to the control group (Retina) (Fig. 4b).

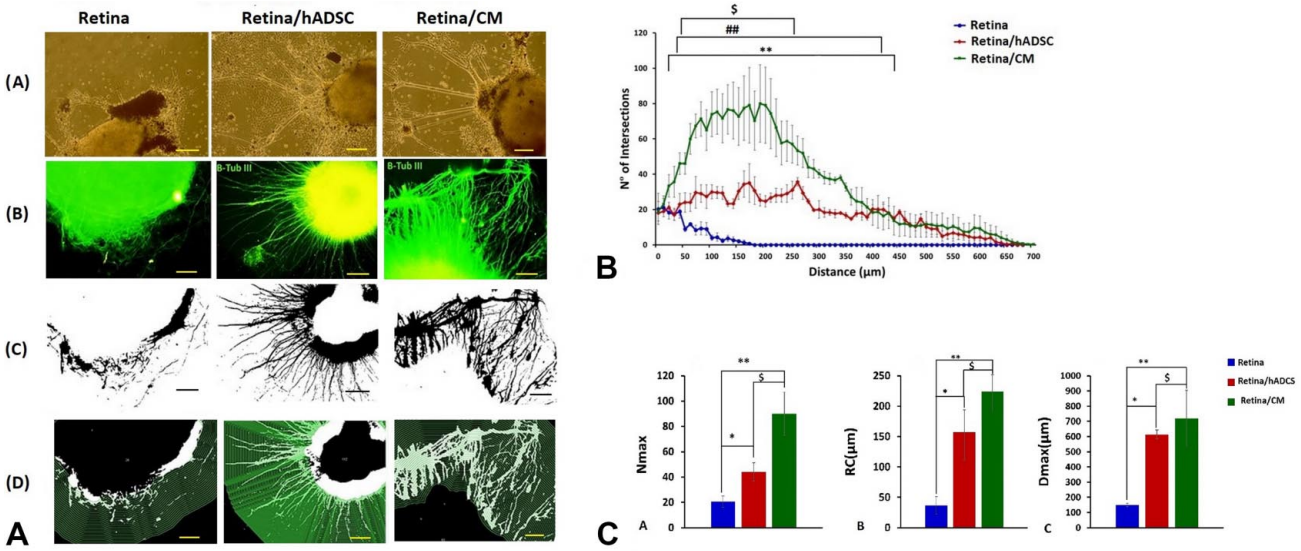

Fig. 3. (a) A: Phase-contrast images of axonal growth. B: Immunofluorescent staining with b-Tub III to determine axonal growth. C and D: Automatic analysis of axonal growth by Image J software in indirect co-culture (Retina+CM), direct co culture (Retina+hADSCs), and control (Retina) groups. (b) Automatic analysis of intersections by ImageJ software, comparison of the number of intersections (processes) in indirect co-culture (Retina+CM), direct co culture (Retina+hADSCs), and control (Retina) groups. ** ($p<0.01$): Comparison of Retina/CM with Retina (control), ## ($p<0.01$): Comparison of Retina/hADSC with control, $ ($p<0.05$): Comparison of Retina/hADSC with Retina/CM. (c) A: Automatic analysis of Nmax (maximum number of processes). B: RC (maximum distance of neuronal processes). C: Dmax (longitudinal growth - maximum length of processes) by ImageJ software in indirect co-culture (Retina+CM), direct co culture (Retina+hADSCs), and control (Retina) groups. * ($p<0.05$) and ** ($p<0.01$): Comparison of Retina/hADSC and Retina/CM groups with Retina (control); $ ($p<0.05$) Comparison of Retina/hADSC with Retina/CM group.

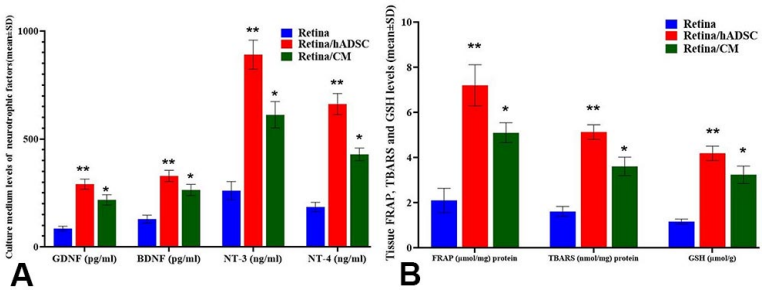

Fig. 4. (a) Culture media levels of glial-derived neurotrophic factor (GDNF), brain-derived neurotrophic factor (BDNF), neurotrophin-3 (NT-3), and NT-4 in indirect co-culture (Retina+CM), direct co culture (Retina+hADSCs), and control (Retina) groups. (b) Cells FRAP, TBARS and GSH levels in indirect co-culture (Retina+CM), direct co culture (Retina+hADSCs), and control (Retina) groups. * (p<0.05) and ** (p<0.01): Comparison of Retina/hADSC and Retina/CM groups with Retina (control) group.

Expression of PTEN, PI3K, AKT and GLUT-4 genes. The relative expression levels of genes associated with the PI3K/AKT pathway were measured to assess the impact of hADSCs and the conditioned media secreted by them on pathway activation. It was observed that both hADSCs and their CM were able to stimulate and enhance this pathway. In the direct co-culture group (Retina + hADSCs), there was a significant increase in the expression of all four genes involved in this pathway (PTEN, PI3K, AKT and GLUT-4) compared to the control group (Retina; p<0.01). Similarly, in the indirect co-culture group (Retina + CM), the evaluation of gene expression in this pathway revealed a significant increase in the expression of PTEN, PI3K, AKT, and GLUT-4 compared to the control group (Retina; p<0.05) (Fig. 5a).

Expression of PTEN, PI3K, AKT and GLUT-4 proteins. Upon evaluating the proteins involved in the neurogenesis process within the PI3K/AKT pathway, it was observed that in the direct co-culture group (Retina + hADSCs), there was a significant increase in the expression of pathway-associated proteins (PTEN, PI3K, AKT and GLUT-4) compared to the control group (Retina; p<0.01). Similarly, in the indirect co-culture group (Retina + CM), the expression of all four proteins (PTEN, PI3K, AKT and GLUT-4) within the PI3K/AKT pathway significantly increased compared to the control group (Retina; p<0.05) (Fig. 5b, 5c).

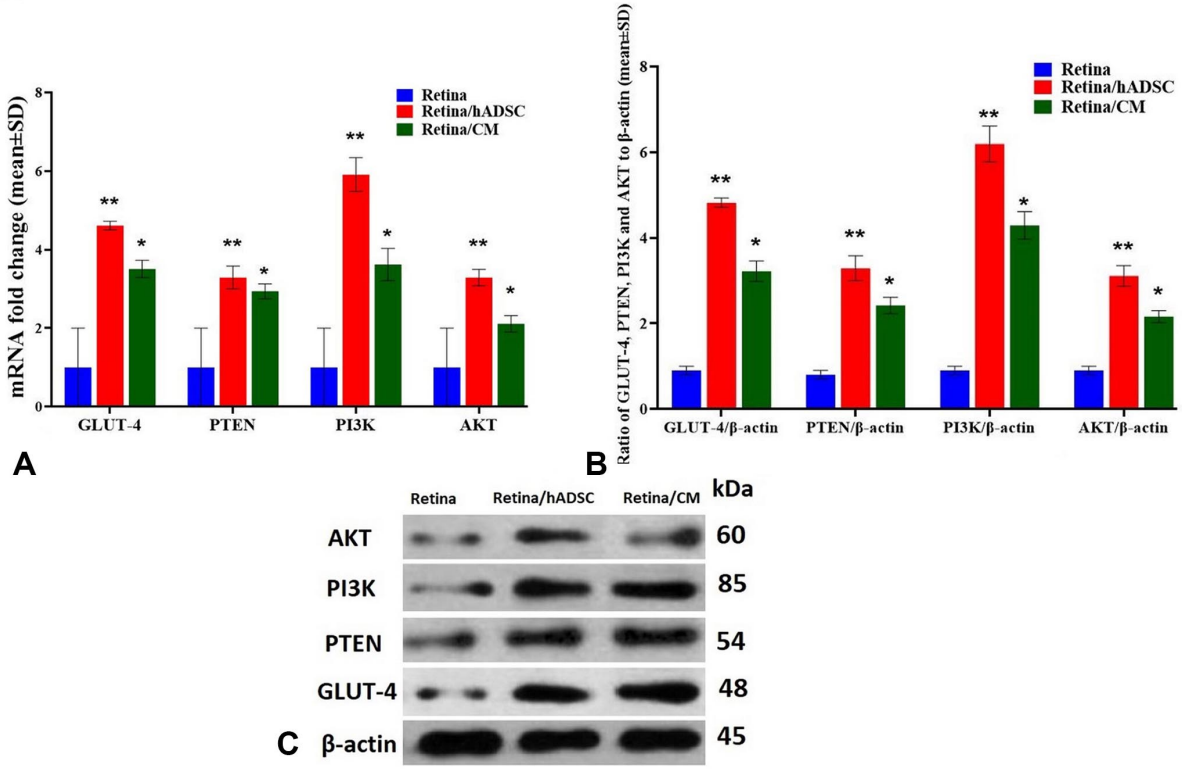

Fig. 5. (a) Cells AKT, PI3K, GLUT-4, and PTEN genes expression in indirect co-culture (Retina+CM), direct co culture (Retina+hADSCs), and control (Retina) groups. Retina (control) group. (b and c) Cells AKT, PI3K, GLUT-4, and PTEN proteins expression to b-actin protein in indirect co-culture (Retina+CM), direct co culture (Retina+hADSCs), and control (Retina) groups. * (p<0.05) and ** (p<0.01): Comparison of Retina/hADSC and Retina/CM groups with Retina (control) group.

DISCUSSION

The findings of this study indicate that co-culturing retinal cells with hADSCs and their conditioned media led to a significant enhancement in the viability of retinal cells. This positive effect may be attributed to the activation of the PI3K/AKT pathway, as demonstrated by the upregulation of genes and proteins including PTEN, PI3K, AKT and GLUT-4. Moreover, co-culturing resulted in increased total antioxidant capacity and elevated levels of neurotrophic factors such as NT-3, BDNF, GDNF and NT-4. These factors may have contributed to the observed improvement in cell viability.

ADSCs are recognized for their ability to secrete a diverse array of growth factors, including NT-3, BDNF, GDNF and NT-4, which have demonstrated effects on nerve function. The observed improvement in viability and proliferation of retinal cells in the co-culture groups and their conditioned medium can be attributed to the secretion of these factors by ADSCs (Ji, 2019). The GDNF, a potent neurotrophic factor, has shown significant effects on dopaminergic neurons, motor neurons, and dorsal root ganglion neurons (Potilinski *et al*., 2020). The NT-4 also exhibits neuroprotective effects by reducing apoptotic factors such as caspase 3 and 9. Additionally, NT-3 enhances the viability of RGCs (Cintrón-Colón *et al*., 2020). In this study, hADSCs were found to elevate the levels of neurotrophic factors NT-3, BDNF, GDNF, and NT-4 in the vicinity of RGCs. To the best of our knowledge, this is the first investigation exploring the impact of hADSCs on retinal cells *in vitro*. These findings suggest that hADSCs have the potential to enhance the survival and functionality of retinal cells through the secretion of various neurotrophic factors.

The findings of the study also showed that co-culture of retinal cells with hADSCs and their CM improved axonal growth. Following axonal cut or pressure on the optic nerve, the transfer of neurotrophic factors through the axonal path is lost, leading to disturbed axonal growth and ganglion cell regeneration. In this study, axonal growth was significantly increased in the co-culture group compared to the control group, which may be due to the secretory factors of hADSCs. The use of hADSCs has previously been shown to improve the regeneration and growth of peripheral neural axons. hADSCs can stimulate neural regeneration through the expression of specific neurotrophic genes and genes related to extracellular matrix proteins required for neuronal growth and myelin synthesis (Lopatina *et al*., 2019; Gong *et al*., 2021). This study confirms the effect of neurotrophic factors secreted by hADSCs on nerve cells. hADSCs can prevent the formation of reactive oxygen species (ROS) and fibrotic tissue in axons by releasing neurotrophic factors, which consequently improves the viability and regeneration of neurons (Wang *et al*., 2020). The results of the present study suggest that hADSCs can potentially be used as a therapeutic approach for promoting axonal growth and regeneration in various neurodegenerative diseases and injuries. The ROS are active free radicals such as superoxide (•O-2), hydroxyl (•OH), and hydrogen peroxide (H2O2), which are created following tissue damage by damaged cells. These free radicals induce apoptosis and inhibit proliferation/ differentiation of neuronal cells through the activation of Bax/Bcl-2/p53 mitochondrial apoptosis pathways and suppression of the PI3K/AKT pathway (Matschke *et al*., 2019). The ROS, in addition to increasing lipid peroxidation of neurons, cause destruction of the myelin sheath and axonal transmission of nerve signals. Studies have shown that these active species inhibit the synthesis of neurotrophic factors and cause anterograde (Wallerian) or retrograde neuronal degeneration (Leyane *et al*., 2022). In addition to activating endogenous antioxidant enzymes of neuronal cells, hADSCs can protect neuronal cells against ROS oxidative damage through their antioxidant enzymes (Park *et al*., 2020). In the present study, hADSCs and their CM were able to increase total antioxidant capacity (FRAP levels) and GSH, while reducing lipid peroxidation levels (TBARS) compared to the control (Retina) group.

Previous studies have indicated that neurotrophic factors such as NT-3, NT-4, FGF and GDNF can influence the axonal growth of ganglion cells *in vitro*. However, *in vivo* studies have demonstrated that only CNTF induces axonal growth in these cells (Joly *et al*., 2017). Nonetheless, hADSCs show promise in addressing these limitations by producing neurotrophic factors that impact BDNF, GDNF, and LIF as paracrine signals, thus potentially preventing the inhibition of axonal growth (Tetri *et al*., 2020). The secretion of BDNF and GDNF by hADSCs can synergistically enhance axonal growth, activating mitogenic protein kinase pathways in retinal ganglion cells. This effect may lead to axonal regeneration and growth in neurons with severed axons (Marconi *et al*., 2012). Studies investigating the effects of factors secreted by hADSCs on axonal growth in various nerves have supported these findings. For instance, hADSCs have been shown to induce axonal growth and sprouting in damaged neurons by releasing BDNF in crushed sciatic nerves, resulting in increased axonal growth and the viability of ganglion cells (Pearse *et al*., 2004).

CONCLUSION

Our study findings demonstrate that hADSCs exhibit promising potential in promoting the axonal growth and survival of retinal ganglion cells. These effects are mediated through a range of mechanisms, including anti-inflammatory

and anti-apoptotic actions, paracrine stimulation, and activation of the PI3K/Akt pathway. The implications of these findings are particularly significant in the context of treating various neurodegenerative diseases and injuries that involve the retina and optic nerve. To fully comprehend the underlying mechanisms responsible for the observed effects of hADSCs on axonal growth and survival, further comprehensive investigations are required. Additionally, optimizing the therapeutic application of hADSCs for promoting axonal regeneration *in vivo* is a crucial area for future research. Nevertheless, our present study offers valuable insights into the potential of hADSCs as a therapeutic approach for addressing eye diseases and other neurodegenerative conditions.

Ethics approval and consent to participate. The ethics committee of the second affiliated hospital of Qiqihar Medical University, Qiqihar Heilongjiang, China supervised the maintenance, behaviour and sacrifice under national and international standards protocols according to NIH Publication, 1996 and European Communities Council Directive of November 24, 1986 (approval number: 2022-kj0076578).

MI, G.; LI, B.; GONG, X.; WU, J.; ZHANG, Y.; MA, L. & SHENG, L. Las células madre derivadas de tejido adiposo humano promueven el crecimiento axonal y la supervivencia de las células ganglionares de la retina de rata mediante estimulación antiinflamatoria, antioxidante, antiapoptótica y paracrina a través de la vía PI3K/Akt. *Int. J. Morphol., 42(6)*:1464-1473, 2024.

RESUMEN: El presente estudio tuvo como objetivo investigar el efecto *in vitro* de las células madre derivadas de tejido adiposo humano (hADSC) y sus secreciones sobre la viabilidad de las células de la retina y el crecimiento axonal. Después del aislamiento, la retina de la rata se mantuvo en recipientes cubiertos con poli-D-lisina/laminina, después de preparar el sobrenadante de las hADSC, se co-cultivaron la retina junto con las células y el medio acondicionado (CM) de las hADSC. La viabilidad se evaluó mediante el ensayo de bromuro de 3-[4,5-dimetiltiazol-2-il]-2,5 difenil tetrazolio (MTT) los días 1, 7 y 14, y el crecimiento axonal de las células de la retina se analizó mediante el software Image J utilizando el complemento Neurite J. La expresión de los genes de la vía PI3K/Akt y sus proteínas se evaluaron mediante reacción en cadena de la polimerasa (PCR) en tiempo real y transferencia Western, respectivamente. Los efectos antioxidantes de las hADSC y su CM se evaluaron midiendo el nivel de sustancia reactiva al ácido tiobarbitúrico (TBARS), capacidad reductora férrica del plasma (FRAP) y glutatión (GSH) en las células de la retina. El factor neurotrófico derivado del cerebro (BDNF), la neurotrofina-3 (NT-3) y la NT-4 en el CM se midieron mediante un ensayo inmunoabsorbente ligado a enzimas (ELISA). El CM contenía altos niveles de BDNF, NT-3 y NT-4 en comparación con el grupo control. La expresión de genes y proteínas de la vía PI3K/Akt junto con los niveles de TBARS, FRAP y GSH también aumentaron en el grupo de hADSC y sus CM en comparación con el grupo control. Los resultados de este estudio mostraron que las hADSC pueden aumentar el crecimiento axonal y la supervivencia de las células de la retina de rata a través de la estimulación antiinflamatoria, antiapoptótica y paracrina, así como a través de la vía PI3K/Akt.

PALABRAS CLAVE: Células madre derivadas de tejido adiposo; Retina; Antioxidante; Vía PI3K/Akt; Cocultivo.

REFERENCES

Achberger, K.; Haderspeck, J. C.; Kleger, A. & Liebau, S. Stem cell-based retina models. *Adv. Drug Deliv. Rev., 140*:33-50, 2019.

Ahmed, Z.; Morgan-Warren, P. J.; Berry, M.; Scott, R. A. & Logan, A. Effects of siRNA-mediated knockdown of GSK3b on retinal ganglion cell survival and neurite/axon growth. *Cells, 8(9)*:956, 2019.

Aladdad, A. M. & Kador, K. E. Adult stem cells, tools for repairing the retina. *Curr. Ophthalmol. Rep., 7(1)*:21-9, 2019.

Bakiu, R.; Pacchini, S.; Piva, E.; Schumann, S.; Tolomeo, A. M.; Ferro, D.; Irato, P. & Santovito, G. Metallothionein expression as a physiological response against metal toxicity in the striped rockcod Trematomus hansoni. *Int. J. Mol. Sci., 23(21)*:12799, 2022.

Cintrón-Colón, A. F.; Almeida-Alves, G.; Boynton, A. M. & Spitsbergen, J. M. GDNF synthesis, signaling, and retrograde transport in motor neurons. *Cell Tissue Res., 382(1)*:47-56, 2020.

Curcio, M. & Bradke, F. Axon regeneration in the central nervous system: facing the challenges from the inside. *Annu. Rev. Cell Dev. Biol., 34*:495-521, 2018.

Dezfuly, A. R.; Safaee, A.; Amirpour, N.; Kazemi, M.; Ramezani, A.; Jafarinia, M.; Dehghani, A. & Salehi, H. Therapeutic effects of human adipose mesenchymal stem cells and their paracrine agents on sodium iodate induced retinal degeneration in rats. *Life Sci., 300*:120570, 2022.

Eastlake, K.; Luis, J. & Limb, G. A. Potential of Müller glia for retina neuroprotection. *Curr. Eye Res., 45(3)*:339-48, 2020.

Fuoco, N. L.; de Oliveira, R. G.; Marcelino, M. Y.; Stessuk, T.; Sakalem, M. E.; Medina, D. A. L.; Modotti, W. P.; Forte, A. & Ribeiro-Paes, J. T. Efficient isolation and proliferation of human adipose-derived mesenchymal stromal cells in xeno-free conditions. *Mol. Biol. Rep., 47(4)*:2475-86, 2020.

George, S.; Hamblin, M. R. & Abrahamse, H. Photobiomodulation-induced differentiation of immortalized adipose stem cells to neuronal cells. *Lasers Surg. Med., 52(10)*:1032-40, 2020.

Gong, Y.; Chen, J.; Jin, Y.; Wang, C.; Zheng, M. & He, L. GW9508 ameliorates cognitive impairment via the cAMP-CREB and JNK pathways in APPswe/PS1dE9 mouse model of Alzheimer's disease. *Neuropharmacology, 164*:107899, 2020.

Han, Q.; Xie, Y.; Ordaz, J. D.; Huh, A. J.; Huang, N.; Wu, W.; Liu, N.; Chamberlain, K. A.; Sheng, Z. H. & Xu, X. M. Restoring cellular energetics promotes axonal regeneration and functional recovery after spinal cord injury. *Cell Metab., 31(3)*:623-41, 2020.

Huang, F.; Chen, J.; Wang, J.; Zhu, P. & Lin, W. Palmitic acid induces microRNA-221 expression to decrease glucose uptake in HepG2 cells via the PI3K/AKT/GLUT4 pathway. *Biomed Res. Int., 2019*:8171989, 2019.

Hunsberger, J.; Austin, D. R.; Henter, I. D. & Chen, G. The neurotrophic and neuroprotective effects of psychotropic agents. *Dialogues Clin. Neurosci., 11(3)*:333-48, 2022.

Ibán-Arias, R.; Lisa, S.; Poulaki, S.; Mastrodimou, N.; Charalampopoulos, I.; Gravanis, A. & Thermos, K. Effect of topical administration of the microneurotrophin BNN27 in the diabetic rat retina. *Graefes Arch. Clin. Exp. Ophthalmol., 257(11)*:2429-36, 2019.

Ji, W. C. Construction of adipose-derived stem cells line that can stably express brain-derived neurotrophic factor and neurotrophin-3 genes and its significance. *J X.i'an Jiaotong Univ. (Med. Sci.), (6)*:393-8, 2019.

Joly, S.; Dalkara, D. & Pernet, V. Sphingosine 1-phosphate receptor 1 modulates CNTF-induced axonal growth and neuroprotection in the mouse visual system. *Neural Plast., 2017*:6818970 , 2017.

Karagiannis, P.; Takahashi, K.; Saito, M.; Yoshida, Y.; Okita, K.; Watanabe, A.; Inoue, H.; Yamashita, J. K.; Todani, M.; Nakagawa, M.; *et al*. Induced pluripotent stem cells and their use in human models of disease and development. *Physiol. Rev., 99(1)*:79-114, 2019.

Koh, A. E.; Alsaeedi, H. A.; Rashid, M. B. A.; Lam, C.; Harun, M. H. N.; Saleh, M. F. B. M.; Luu, C. D.; Kumar, S. S.; Ng, M. H.; Isa, H. M.; *et al*. Retinal degeneration rat model: A study on the structural and functional changes in the retina following injection of sodium iodate. *J. Photochem. Photobiol. B, 196*:111514, 2019.

Leyane, T. S.; Jere, S. W. & Houreld, N. N. Oxidative Stress in ageing and chronic degenerative pathologies: Molecular mechanisms involved in counteracting oxidative stress and chronic inflammation. *Int. J. Mol. Sci., 23(13)*:7273, 2022.

Lopatina, T.; Kalinina, N.; Karagyaur, M.; Stambolsky, D.; Rubina, K.; Revischin, A.; Pavlova, G.; Parfyonova, Y. & Tkachuk, V. Correction: adipose-derived stem cells stimulate regeneration of peripheral nerves: BDNF secreted by these cells promotes nerve healing and axon growth de novo. *PLoS One, 14(7)*:e0219946, 2019.

Marconi, S.; Castiglione, G.; Turano, E.; Bissolotti, G.; Angiari, S.; Farinazzo, A.; Constantin, G.; Bedogni, G.; Bedogni, A. & Bonetti, B. Human adipose-derived mesenchymal stem cells systemically injected promote peripheral nerve regeneration in the mouse model of sciatic crush. *Tissue Eng. Part A., 18(11-12)*:1264-72, 2012.

Matschke, V.; Theiss, C. & Matschke, J. Oxidative stress: The lowest common denominator of multiple diseases. *Neural Regen. Res., 14(2)*:238, 2019.

Metcalfe, S. M. Neuroprotective immunity: leukaemia inhibitory factor (LIF) as guardian of brain health. *Med. Drug Discov., 2*:100006, 2019.

Ong, W. K.; Chakraborty, S. & Sugii, S. Adipose tissue: understanding the heterogeneity of stem cells for regenerative medicine. Biomolecules, 11(7):918, 2021.

Packer, J. D.; Chang, W. T. & Dragoo, J. L. The use of vibrational energy to isolate adipose-derived stem cells. *Plast. Reconstr. Surg. Glob. Open, 6(1)*:e1620, 2018.

Park, J. S.; Piao, J.; Park, G. & Hong, H. S. Substance-P restores cellular activity of ADSC impaired by oxidative stress. *Antioxidants (Basel), 9(10)*:978, 2020.

Pearse, D. D.; Pereira, F. C.; Marcillo, A. E.; Bates, M. L.; Berrocal, Y. A.; Filbin, M. T. & Bunge, M. B cAMP and Schwann cells promote axonal growth and functional recovery after spinal cord injury. *Nat. Med., 10(6)*:610-6, 2004.

Pereiro, X.; Ruzafa, N.; Acera, A.; Fonollosa, A.; Rodriguez, F. D. & Vecino, E Dexamethasone protects retinal ganglion cells but not Müller glia against hyperglycemia *in vitro. PLoS One, 13(11)*:e0207913, 2018.

Potilinski, M. C.; Lorenc, V.; Perisset, S. & Gallo, J. E. Mechanisms behind retinal ganglion cell loss in diabetes and therapeutic approach. *Int. J. Mol. Sci., 21(7)*:2351, 2020.

Prendergast, E. N.; de Souza Fonseca, M. A.; Dezem, F. S.; Lester, J.; Karlan, B. Y.; Noushmehr, H.; Lin, X. & Lawrenson, K. Optimizing exosomal RNA isolation for RNA-Seq analyses of archival sera specimens. *PLoS One, 13(5)*:e0196913, 2018.

Skaper, S. D. Neurotrophic factors: an overview. *Methods Mol .Biol., 1727*:1-17, 2018.

Tetri, L. H.; Kolla, V.; Golden, R. L.; Iyer, R.; Croucher, J. L.; Choi, J. H.; Macfarland, S. P.; Naraparaju, K.; Guan, P.; Nguyen, F.; *et al*. RET receptor expression and interaction with TRK receptors in neuroblastomas. *Oncol. Rep., 44(1)*:263-72, 2020.

Verma, M. K.; Jaiswal, A.; Sharma, P.; Kumar, P. & Singh, A. N. Oxidative stress and biomarker of TNF-α, MDA and FRAP in hypertension. *J. Med. Life, 12(3)*:253, 2019.

Wang, H.; Zheng, Z.; Han, W.; Yuan, Y.; Li, Y.; Zhou, K.; Wang Q, Xie L, Xu K, Zhang H. Metformin promotes axon regeneration after spinal cord injury through inhibiting oxidative stress and stabilizing microtubule. *Oxid. Med. Cell Longev., 2020*: +9741369, 2020.

Ye, L.; Ni, X.; Zhao, Z. A.; Lei, W. & Hu, S. The application of induced pluripotent stem cells in cardiac disease modeling and drug testing. *J. Cardiovasc. Transl. Res., 11(5)*:366-74, 2018.

Zakrzewski, W.; Dobrzynski, M.; Szymonowicz, M. & Rybak, Z. Stem cells: past, present, and future. *Stem Cell Res. Ther., 10(1)*:1-22, 2019.

Zhao, P.; Li, X.; Li, Y.; Zhu, J.; Sun, Y. & Hong, J. Mechanism of miR-365 in regulating BDNF-TrkB signal axis of HFD/STZ induced diabetic nephropathy fibrosis and renal function. *Int. Urol. Nephrol., 53(10)*:2177-87, 2021.

Zuo, Z.; Ji, S.; He, L.; Zhang, Y.; Peng, Z. & Han, J. LncRNA TTN-AS1/miR-134-5p/PAK3 axis regulates the radiosensitivity of human large intestine cancer cells through the P21 pathway and AKT/GSK-3b/b-catenin pathway. *Cell Biol. Int., 44(11)*:2284-92, 2020.

Corresponding author:
Lijie Sheng
Department of Ophthalmology
The Second Affiliated Hospital of Qiqihar Medical University
Qiqihar Heilongjiang 161006
CHINA

E-mail: lijiesheng@qmu.edu.cn